MOLECULAR AND CELLULAR BIOLOGY, Nov. 1985, p. 2903–2912
0270-7306/85/112903-10$02.00/0

Vol. 5, No. 11

Growth-Dependent Synthesis of c-*myc*-Encoded Proteins: Early Stimulation by Serum Factors in Synchronized Mouse 3T3 Cells

HÅKAN PERSSON,[1]†* HARRY E. GRAY,[2]† AND FRANCOIS GODEAU[2]‡

Department of Genetics,[1] and Department of Pharmacology, Harvard Medical School, and Division of Cell Growth and Regulation, Dana-Farber Cancer Institute,[2] Boston, Massachusetts 02115

Received 30 April 1985/Accepted 27 July 1985

Synthesis of the c-*myc* gene product was measured during the entire cell cycle of subconfluent mouse 3T3 cells with an antibody raised against a human c-*myc* synthetic peptide. The antiserum recognized two mouse c-*myc*-encoded proteins with apparent molecular weights in sodium dodecyl sulfate-polyacrylamide gels of 62,000 and 60,000. Cell-derived p62 was compared with the mouse c-*myc* gene product synthesized in vitro. Immunoprecipitation, electrophoretic analyses, and peptide mapping provided evidence that p62 is encoded by the mouse c-*myc* gene. The rate of synthesis of the c-*myc* proteins was tightly coupled to the cellular growth state of nontransformed A31 3T3 cells, but not to that of their benzo(a)pyrene-transformed derivative (BPA31). Furthermore, the synthesis of the c-*myc* proteins was stimulated by the exposure of confluent, density-arrested A31 cells to platelet-derived growth factor or fibroblast growth factor. Tightly synchronized cell populations were obtained on the addition of serum factors to subconfluent, serum-deprived A31 cells, and c-*myc* expression could be monitored for more than one complete cell cycle. One hour after stimulation the steady-state level of the 2.2 kilobase c-*myc* transcript increased 30-fold relative to that of quiescent cells and decreased thereafter to the level observed during exponential growth. The rate of synthesis of c-*myc*-encoded proteins was determined by immunoprecipitation after a 2-h labeling period. After an initial sevenfold increase detectable 2 h after serum addition, the rate of synthesis remained constant throughout the rest of the cell cycle. No further changes associated with the late prereplicative period, S phase, G_2, or mitosis could be demonstrated. Pulse-chase and long-term labeling experiments revealed different half-lives for the two c-*myc*-encoded proteins. The half-lives of the c-*myc* proteins, however, were independent of the cellular growth state. The sustained expression observed throughout the cell cycle suggests that the growth-related function of c-*myc* may be required during the G_0-G_1 transition and in all phases of the cycle of the growing cell.

The avian defective acute leukemia viruses contain a gene, v-*myc*, the product of which transforms hematopoietic cells and fibroblasts in culture (7). The cellular homolog of this gene, c-*myc*, is strongly conserved in vertebrate evolution (7) and is expressed ubiquitously in a variety of tissues (45). Like other homologs of viral oncogenes, the c-*myc* proto-oncogene is thought to play an important role in the control of proliferation in normal cells. Indeed, both the positive correlation between c-*myc* expression and cellular growth state and the responsiveness of c-*myc* expression to mitogenic stimulation substantiate this thesis (10, 26). Furthermore, inappropriate expression of the c-*myc* gene can lead to a relaxation in growth factor requirements in cultured cells (4) or to increased susceptibility of the adult animal to the development of tumors following its introduction into the mouse germ line (46). Deregulation of c-*myc* expression therefore could contribute to malignant transformation. Accordingly, alterations in the c-*myc* proto-oncogene have been found in association with avian, murine, and human malignancies (7). These changes include gene amplification (12, 14, 30) and altered c-*myc* transcriptional activity. The latter can result from retroviral promoter (long terminal repeat) integration in the vicinity of the c-*myc* gene (24) or from a chromosomal rearrangement that places the c-*myc* gene under the control of regulatory sequences proper to the immunoglobulin locus, as seen in Burkitt's lymphoma and mouse plasmacytomas (29). It has been suggested that the c-*myc* gene product performs an immortalizing function (28), but its precise role in cell physiology remains elusive.

Little is known about the proteins encoded by the c-*myc* gene, and antibodies raised against c-*myc* gene products or sequences have only recently been described (3, 9, 21, 22, 34, 38). Like the virally encoded v-*myc*-transforming proteins (1, 9, 15, 16), the c-*myc* gene product is a nuclear, DNA-binding protein (16, 35). The antibodies described thus far recognize two or possibly three structurally related human proteins with an approximate molecular weight of 65,000 in sodium dodecyl sulfate (SDS)-polyacrylamide gels (22, 34, 38). The c-*myc* proteins appear to be phosphorylated (22, 38), but no particular function in cellular growth has been ascribed to them. These considerations emphasize the need for additional studies that attempt to relate c-*myc* expression to normal cellular events. The use of an antibody has the advantage over the use of hybridization probes of being able to explore more than one parameter of gene expression. Thus, information can be gained on the rate of synthesis, the stability, the possible posttranslational modifications, and the subcellular localization of the active gene products. With these considerations in mind, we measured the expression of c-*myc* throughout the 3T3 cell cycle using both a hybridization probe and an antibody raised against the human c-*myc* gene product.

We report here that the mouse c-*myc* gene directs the synthesis of at least two polypeptides, $p60^{c\text{-}myc}$ and $p62^{c\text{-}myc}$. Their rates of synthesis are correlated with growth and are increased by the application of platelet-derived growth fac-

* Corresponding author.
† Present address: Department of Medical Genetics, Uppsala University, The Biomedical Center, S-751 23 Uppsala, Sweden.
‡ Present address: UA Centre National de la Recherche Scientifique, 040557, Institut Pasteur, 75724 Paris, Cedex 15 France.

tor (PDGF) to confluent A31 3T3 cells. When examined throughout the BALB/c 3T3 cell division cycle, the rates of synthesis of the c-*myc* proteins increase rapidly only in the early prereplicative period that follows serum stimulation of subconfluent quiescent cells. $p62^{c\text{-}myc}$ is a relatively stable protein that decays with a half-life longer than 6 h, whereas $p60^{c\text{-}myc}$ is unstable.

MATERIALS AND METHODS

Cell lines, cell culture conditions, and growth factors. Mouse BALB/c 3T3 cells (clone A31) and their benzo(a)pyrene-transformed derivative (BPA31) (25) were maintained in 75-cm^2 tissue culture flasks (Becton Dickinson Labware, Oxnard, Calif.) in the Dulbecco modification of Eagle minimal medium (DME) supplemented with 3.7 g of sodium bicarbonate per liter, 4 mM glutamine, and 10% calf serum (Flow Laboratories, Inc., McLean, Va.). Cultures were incubated at 37°C in a water-saturated atmosphere containing 10% CO_2. Fresh cell cultures were initiated frequently from frozen stocks (every 6 to 8 weeks) and assayed routinely for the absence of contaminating mycoplasma (41). Cell numbers were determined by counting duplicate trypsinized cultures in a Coulter Counter (Coulter Electronics, Inc., Hialeah, Fla.). Partially purified PDGF and purified fibroblast growth factor (FGF) were kindly provided by C. Stiles (Harvard Medical School, Boston) and D. Gospodarowicz (University of California, San Francisco), respectively.

Cell synchronization. To generate quiescent cultures that could be stimulated to reenter the cell cycle synchronously, the BALB/c A31 cells were seeded at a density of 1,700 cells per cm^2 in the maintenance medium in 100-mm dishes (Becton Dickinson Labware) coated with poly-D-lysine as described previously (30). Unrestricted growth was permitted until the cell density reached 10^4 cells per cm^2 (approximately 2 days). At this time serum starvation was initiated by reducing the serum concentrations to 0.5% in DF31 medium following one rinse with unsupplemented DME. DF31 medium was a mixture of 3 parts DME and 1 part Ham F12 medium supplemented with 15 mM *N*-2-hydroxyethylpiperazine-*N'*-2-ethanesulfonic acid (pH 7.35), 1.6 g of histidine per liter, 2.5 μM ethanolamine, 4 mM glutamine, and trace elements (including selenium) as described previously (40, 42). After 24 h the medium was again aspirated and replaced by DF31, containing 0.5% platelet-poor human plasma (PPP) instead of calf serum, for an additional 18 h of incubation. PPP was prepared and tested on cultures of density-arrested A31 cells for mitogenicity and for the absence of toxicity essentially as described previously (36).

At the end of the starvation period (during which cell loss was moderate but tolerable) the viable cells had assumed a flattened morphology, and they remained subconfluent at a density of 25,000 cells per cm^2. Synchronous growth was initiated by restoring fresh DF31 medium supplemented with 10% calf serum to the quiescent cultures. Growth arrest of the chemically transformed BPA31 cells by serum deprivation was achieved by using the same protocol, except that serum and PPP concentrations were reduced to 0.2%, and the total starvation period was extended to 72 h (instead of 42 h).

A state of quiescent growth arrest was also achieved by allowing confluent monolayers of A31 cells to become density-arrested in DME containing 10% calf serum. Two days after cells reached confluence the medium was changed to DME supplemented with 5% PPP. After an additional 24-h period these monolayers were labeled in vivo with [^{35}S]methionine (50 μCi/ml) (34) either without further treatment (as controls) or following exposure to individual growth factors.

The cellular growth state was monitored by flow microfluorometry and by measuring the incorporation of [^{3}H]thymidine (1 μCi/ml, 80 Ci/mmol, in DME) into trichloroacetic acid (TCA)-insoluble material. Cells were incubated at 37°C for 1 h in the presence of the labeled precursor and fixed in cold 10% TCA containing 1 mM unlabeled thymidine. After three washings with 10% TCA and three washings with cold methanol, fixed cultures were either processed for autoradiography (44) or dissolved in 0.1 M NaOH containing 1% SDS and 1 mM EDTA and then precipitated with 10% TCA. Precipitates were collected on Whatman GF/C filters, which were washed and counted by liquid scintillation spectroscopy.

Analysis of in vitro-synthesized c-*myc* transcripts and translation products. A full-length mouse c-*myc* cDNA clone (43) was inserted into the *Hin*dIII site of the pSp64 M13 polylinker (Promega Biotech). The resulting plasmid pSpmyc-2 was linearized with *Eco*RI and transcribed in vitro with the phage SP6 RNA polymerase (19). RNA isolated from the in vitro transcription system was capped with guanylyl transferase (Bethesda Research Laboratories, Gaithersburg, Md.) and then translated in a rabbit reticulocyte cell-free system in the presence of [^{35}S]methionine. The total cell-free translation products were either analyzed on 10% SDS-polyacrylamide gels or immunoprecipitated with a human c-*myc* peptide antiserum (34) and then analyzed by SDS-polyacrylamide gel electrophoresis (PAGE). The c-*myc*-encoded proteins synthesized in vitro were isolated from the SDS-polyacrylamide gel by electroelution in the presence of carrier bovine serum albumin. Electroeluted proteins were reduced, alkylated, and then digested with pepsin (2). The amount of pepsin and the duration of the partial digestion (18 h with 2.5 μg of pepsin [Sigma Chemical Co., St. Louis, Mo.] per ml) were adjusted to optimize the number of ^{35}S-labeled peptides available for comparison between different samples. The resulting peptides were separated either by reversed-phase high-pressure liquid chromatography (HPLC) with a C18-RP column (Bio-Rad Laboratories, Richmond, Calif.) or in two dimensions on thin-layer chromatographic plates by electrophoresis in the first dimension followed by ascending chromatography (2). Peptides analyzed in two dimensions on thin-layer plates were visualized by autoradiography. The HPLC column was eluted with a linear gradient of 0 to 49% acetonitrile in 0.1% trifluoroacetic acid in a total time of 80 min. The flow rate was 1.0 ml/min, and 0.5-ml fractions were collected and analyzed by liquid scintillation spectroscopy. Immunoprecipitated p62 synthesized in vitro and cell-derived p62 were analyzed by two-dimensional gel electrophoresis as described by O'Farrell (33).

Cell labeling and immunoprecipitation. Cell monolayers were washed once with DME lacking methionine. They were then labeled at 37°C for the indicated times with [^{35}S]methionine (50 μCi/ml) in medium (either complete or containing reduced concentrations of calf serum or PPP) formulated with DME lacking methionine. Cell extracts were prepared in RIPA buffer (0.5 M Tris hydrochloride [pH 7.5], 0.15 M NaCl, 0.1% sodium dodecyl sulfate, 1% Triton X-100, 0.5% sodium deoxycholate, 1 mM phenylmethylsulfonylfluoride) and immunoprecipitated with the indicated sera as described previously (34). The different conditions within each experiment were compared as indicated by immunoprecipitating either equal quantities of acid-

precipitable radioactivity or quantities of acid-precipitable radioactivity extracted from equal numbers of cells. Washed immunoprecipitates were electrophoresed in 10% SDS-polyacrylamide gels, which were then processed for autoradiography and scanning densitometry as described previously (34).

Extraction and analysis of cellular RNA. Total cellular RNA was prepared by the guanidine isothiocyanate method as described previously (11), and poly(A)$^+$ RNA was isolated from total RNA by chromatography on oligo(dT) cellulose (5). Isolated RNA was electrophoresed in 1% agarose gels containing 0.7% formaldehyde, transferred to nitrocellulose, and hybridized to the indicated nick-translated DNA probes.

RESULTS

c-*myc* encodes p62 and p60, two closely related polypeptides. To gain information on the nature of the proteins encoded by the mouse c-*myc* gene, we first characterized the products obtained in cell-free systems. In vitro transcription was achieved by using the purified Sp6 phage RNA polymerase and its cognate recognition signals (19). The template was obtained by inserting a full-length mouse c-*myc* cDNA clone (43) downstream from the Sp6 phage promoter elements. The in vitro-synthesized transcript was purified and used to program a cell-free translation system derived from rabbit reticulocytes. [^{35}S]methionine-labeled products were then analyzed by SDS-PAGE and fluorography. Two polypeptides with apparent molecular weights of 60,000 and 62,000 in SDS gels were demonstrated (Fig. 1). The mouse c-*myc* in vitro translation products were immunoprecipitated with an antiserum directed against amino acids 24 to 40 of the human c-*myc* protein (34). Both the 62- and the 60-kilodalton (kDa) proteins were specifically recognized by the antibody (Fig. 1), indicating the existence of antigenic determinants shared by the human and murine proteins. There are several possible explanations for the in vitro synthesis of both p60 and p62 from a single gene. Heterogeneity of the mRNA transcribed in vitro, posttranslational modifications, and anomalous protein migration in SDS-PAGE could all contribute to the heterogeneity that we observed. The antibody was then used to immunoprecipitate c-*myc* proteins from extracts of 3T3 cells metabolically labeled with [^{35}S]methionine. Similarly, a 62- and a 60-kDa protein were again specifically recognized (Fig. 1). Cell-derived p60 migrated slightly less rapidly in SDS-PAGE than did p60 synthesized in vitro (Fig. 1), suggesting possible posttranslational modifications of p60 occurring in vivo but not in vitro.

To further explore the relationship between the p62 and p60 proteins synthesized in vitro, a structural analysis by peptide mapping was undertaken. Gel-purified [^{35}S]methionine-labeled proteins were partially digested with pepsin, and the resulting peptides were separated by fingerprint or reversed-phase HPLC (Fig. 2). Both analyses revealed a structural identity between the two polypeptides, although the relative intensities of the different peptides eluted from the HPLC column showed some variability (possibly resulting from differential recovery between column runs). A similar analysis was undertaken to compare the 3T3 cell-derived, immunoprecipitated p62 protein with p62 synthesized in vitro. (We have not been able to isolate enough purified, radioactively labeled, cell-derived p60 to allow a similar peptide mapping of this protein.)

When separated by HPLC, a majority of the peptides coeluted. With one exception, the remaining peptides showed only minor variations in retention time (Fig. 2B). The major difference between the peptide maps of cell-derived p62 and p62 synthesized in vitro was the absence of one peptide from the cell-derived p62 profile (Fig. 2B, arrow). Such a difference may indicate either differences in the primary structure of cell-derived p62 and p62 synthesized in vitro or a posttranslational modification(s) of the cell-derived p62 not present in the cell-free-synthesized p62. Support for the latter explanation was provided by two-dimensional electrophoretic analysis of cell-derived p62, which demonstrated a broad distribution of isoelectric points centered at pH 6.2 (data not shown), suggesting the presence of posttranslational modifications. In agreement with the close similarity between the peptide maps of cell-derived p62 and p62 synthesized in vitro, the latter analysis also showed

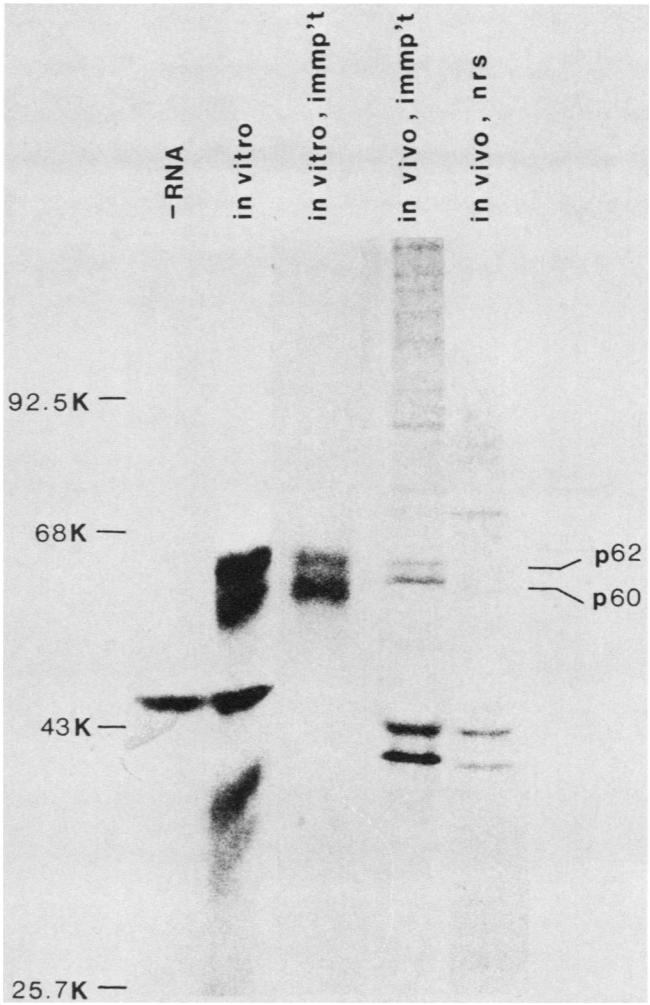

FIG. 1. In vitro and in vivo synthesis of c-*myc* proteins. Mouse c-*myc* RNA was synthesized in a cell-free system with *Eco*RI-restricted plasmid pSpmyc-2 and phage Sp6 RNA polymerase. The RNA was capped and then translated in a rabbit reticulocyte cell-free system, and the translation products were analyzed by SDS-PAGE (in vitro). -RNA denotes that no RNA was added to the cell-free translation system. The cell-free translation products were immunoprecipitated with a c-*myc* peptide serum (in vitro, immp't). Mouse 3T3 cells were pulse-labeled in vivo with [^{35}S]methionine (50 μCi/ml) for 2 h, and the cell extract was immunoprecipitated with the c-*myc* peptide antiserum (in vivo, immp't) or with a preimmune rabbit serum (in vivo, nrs). Numbers to the left of the gels are molecular weights (in thousands [K]).

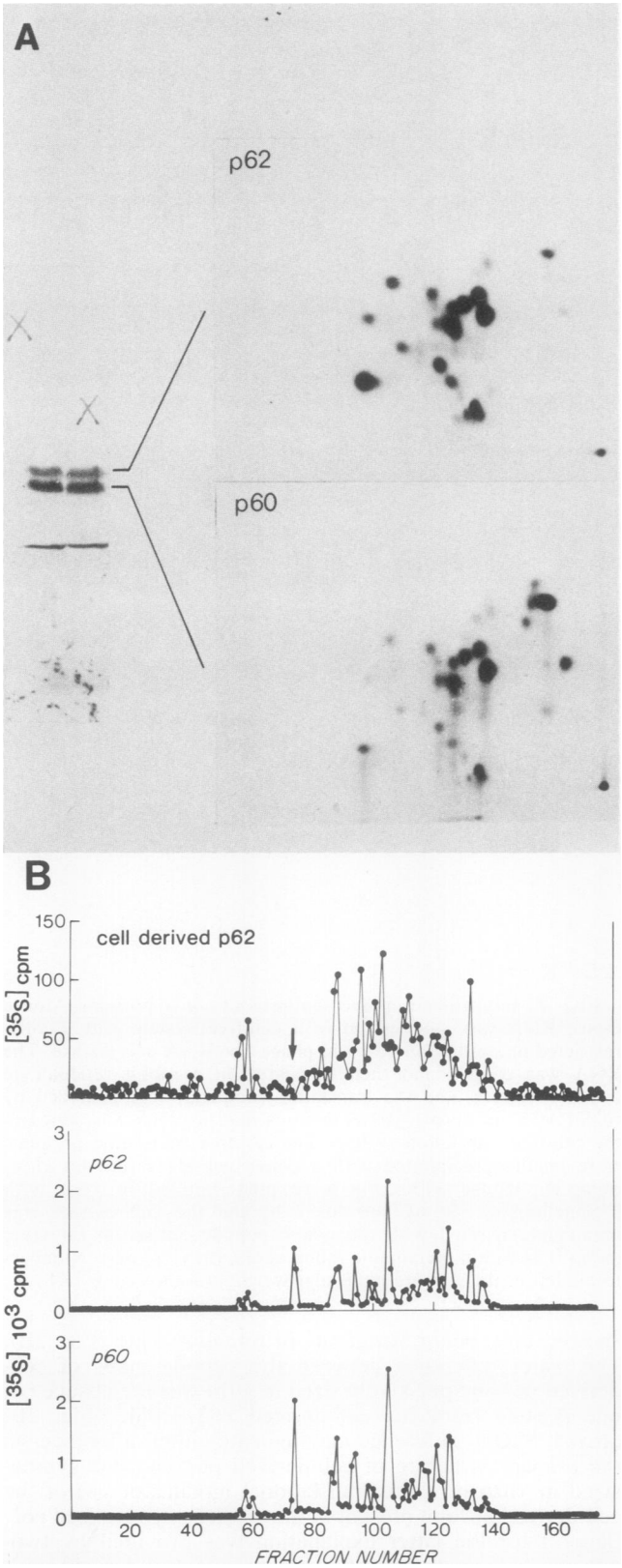

FIG. 2. Peptide analysis of c-*myc* proteins. Cell-free translation products synthesized in response to synthetic, purified mouse c-*myc* mRNA (left side of panel A), and also cell-derived p62 immunoprecipitated from labeled cell extracts (data not shown) were separated on 10% SDS-polyacrylamide gels. They were then electroeluted from the gels and digested with pepsin. [^{35}S]methionine-labeled peptides were separated on thin-layer plates in two dimensions by electrophoresis followed by ascending chromatography (A), or by reversed-phase HPLC with a C18-RP column (B).

an isoelectric point at pH 6.2. Taken together, these results indicate that the mouse c-*myc* gene directs the synthesis of two polypeptides, the apparent molecular weights of which are 62,000 and 60,000 and which are closely related structurally and immunologically.

Synthesis of p62$^{c\text{-}myc}$ correlates with cellular growth state and is PDGF-dependent in A31 cells. Previous studies in which hybridization probes have been used have established a direct relationship between the steady-state level of c-*myc* transcript and the cellular growth state in nontransformed A31 cells, and the down regulation of c-*myc* expression that accompanies cellular quiescence has been found to be markedly diminished in their benzopyrene-transformed derivative BPA31 (10). To determine if these results could be confirmed by studying the synthesis of the c-*myc*-encoded proteins, we compared the rate of synthesis of the c-*myc* proteins in quiescent cells with that of exponentially growing cells in these two cell lines. Growth arrest of subconfluent cells was brought about by serum deprivation. Quiescent and exponentially growing cultures were labeled with [^{35}S]methionine, and extracts were immunoprecipitated with the anti-human c-*myc* antibody (34). Immunoprecipitates were normalized to the total acid-insoluble radioactivity incorporated into the protein. In nontransformed A31 cells p62$^{c\text{-}myc}$ and p60$^{c\text{-}myc}$ were synthesized at a fivefold higher rate in exponentially growing cells than in growth-arrested cells (Fig. 3A and B). In contrast, this down-regulation could not be demonstrated in BPA31 cells, where the growing and quiescent synthetic rates differed only by a factor smaller than two (Fig. 3A and 3B). These results are in agreement with those of previous studies of c-*myc* RNA (10) and indicate that the synthesis of c-*myc* proteins correlates with cell growth in nontransformed A31 cells.

In confluent A31 cells c-*myc* expression has been shown to be highly responsive to stimulation by competence (37) factors such as PDGF (26). Therefore, we examined the effects of PDGF and FGF on the rate of c-*myc* protein synthesis in confluent, growth-arrested A31 cells. Partially purified PDGF and purified FGF both increased the synthesis of p62$^{c\text{-}myc}$ (Fig. 3C). When the long labeling period was reduced to 2 h, a PDGF-induced increase in p60$^{c\text{-}myc}$ synthesis could also be demonstrated (data not shown). Thus, the basic features of c-*myc* RNA accumulation established with hybridization probes could also be demonstrated by studying the synthesis of the c-*myc*-encoded proteins.

Expression of the c-*myc* gene during a complete cell cycle in A31 cells. The observed correlation between cell growth and c-*myc* protein synthesis prompted us to follow the kinetics of both c-*myc* RNA accumulation and c-*myc*-encoded protein synthesis during the entire cell cycle of A31 3T3 fibroblasts. The growth of subconfluent populations of 3T3 cells was arrested by serum deprivation. The removal of serum factors from subconfluent cells resulted in a 100-fold reduction of the thymidine labeling index (from 60 to 0.5%) after a period of 2 days. That cells were arrested with a G_1 DNA content was confirmed by flow microfluorometry (FMF) and by the stationary growth curve (Fig. 4). Following serum stimulation the cells entered S phase in a tightly synchronous fashion as the thymidine labeling index rose sharply from 0.5

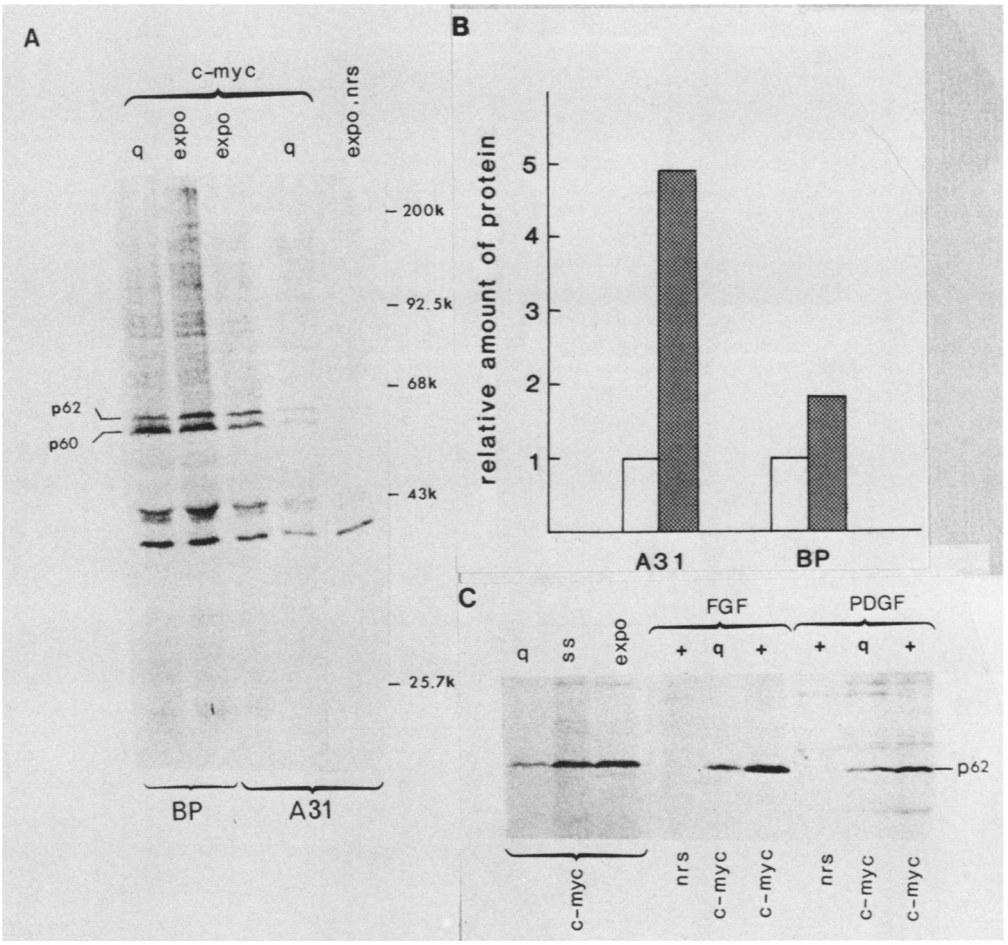

FIG. 3. Synthesis of c-*myc* proteins in quiescent, mitogen-stimulated, and growing cells. Subconfluent serum-starved (q) or exponentially growing (expo) mouse A31 or BPA31 (BP) cells were pulse-labeled with [^{35}S]methionine for 2 h. Cell extracts containing equal amounts of TCA-insoluble radioactivity were immunoprecipitated with a c-*myc* peptide antiserum (c-*myc*) or with a preimmune serum (expo, nrs). (A) Samples were analyzed by SDS-PAGE. Numbers to the right of the gel are molecular weights (in thousands [K]). (B) The resulting fluorogram was scanned with a densitometer for quantitation of the combined rate of synthesis of both c-*myc* proteins. Open column, Quiescent cells; filled column, exponentially growing cells. (C) Subconfluent serum-starved (q) and growing (expo) A31 cells were labeled for 14 h with [^{35}S]methionine, and some quiescent cells were also serum stimulated with complete medium (ss) during the 14-h labeling period. Furthermore, confluent density-arrested cells were exposed to 0.1 ng of FGF or PDGF per ml during a 10-h period of labeling with [^{35}S]methionine. (+) Cell extracts containing equal amounts of radioactivity were immunoprecipitated with either a c-*myc* peptide antiserum (c-*myc*) or a preimmune rabbit serum (nrs). Immune complexes were analyzed by SDS-PAGE and fluorography.

to 40% between 10 and 12 h and reached a maximum of 80% by 17 h after serum addition. At 24 h following serum shift up the labeling index measured by a 1-h thymidine pulse fell dramatically to 20%, while the cumulative labeling index attained 98%. The viability and the responsiveness to serum stimulation of the entire population of cells that remained attached was further documented by the doubling in cell number that was completed by 28 h. FMF analysis confirmed both the high degree of synchrony that was attained and also its persistence beyond mitosis, which occurred at about 25 h (Fig. 4). The sharp decrease in the fraction of cells with a G_2 DNA content observed between 22 and 25 h indicates a synchronous passage through mitosis. Good synchrony persisted into the second cell cycle, since 85% of the cells had a G_1 DNA content 28 h after serum addition.

Total RNA was prepared at different times following serum addition and analyzed by Northern hybridization to a DNA probe containing the entire mouse c-*myc* gene; both total and poly(A)$^+$ RNA was included in the analysis. A large increase in the 2.2-kilobase c-*myc* transcript was observed in the total RNA preparation 1 h after the addition of serum (Fig. 5). At this time the level of c-*myc* transcript was elevated approximately 30-fold over that of quiescent cells (Fig. 5B). The content of the c-*myc* transcript decreased in early G_1 phase and reached a constant level about 10-fold higher than that in quiescent cells about 10 h after serum addition. The analysis of poly(A)$^+$ c-*myc* RNA revealed similar kinetics, except that the degree of stimulation at the earliest measured time (1 h) was not as great (about threefold lower) as that observed for the c-*myc* transcript in the total RNA samples (Fig. 5B), suggesting that a significant fraction of the 2.2-kilobase c-*myc* transcript was not poly(A)$^+$ at early times following serum stimulation. This possibility, however, requires further, systematic investigation. In the middle of the G_1 period the concentration of the poly(A)$^+$ c-*myc* transcript attained a constant level that was maintained throughout the rest of the cell cycle.

In parallel cultures the rate of synthesis of c-*myc* gene products was determined at different times following serum restoration by immunoprecipitation of extracts from cells

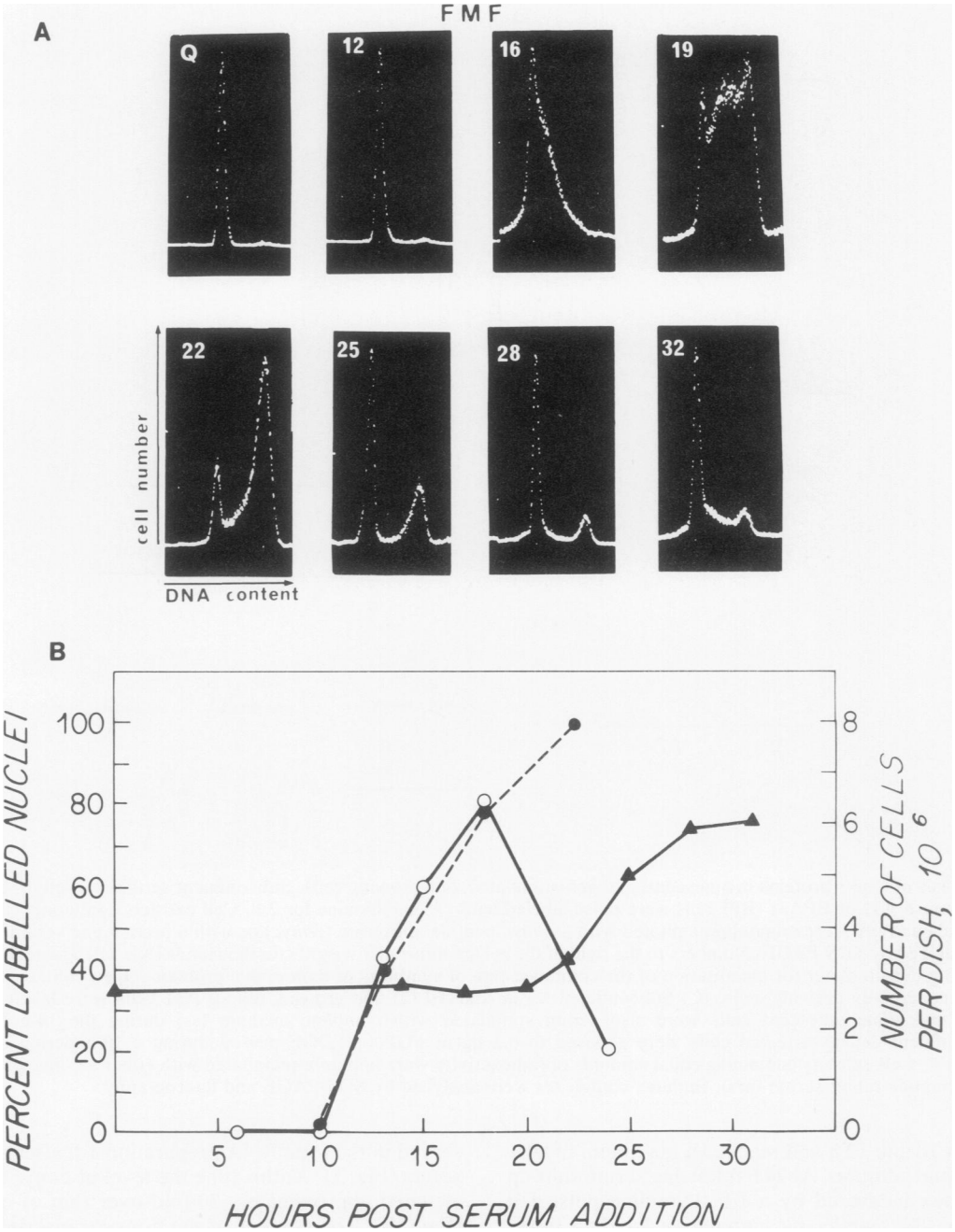

FIG. 4. Progression of quiescent serum-starved A31 3T3 cells through the cell cycle after serum stimulation. Subconfluent mouse 3T3 cells (clone A31) were made quiescent by serum starvation as described in the text. At the end of the starvation period more than 98% of the cells were quiescent as shown by FMF (A) or pulse-labeling with [^{3}H]thymidine (B). Fresh complete medium containing 10% calf serum was added at time zero, and cell cycle progression was monitored by FMF and by incorporation of [^{3}H]thymidine followed by autoradiography. The labeled precursor was either added at the indicated time and left for 1 h before fixation (○) or added at the time of serum restoration and fixed at the indicated time (●). Fixation was followed by autoradiographic determination of the labeling index. Cell number was determined throughout the experiment (▲) with a Coulter Counter.

that were pulse-labeled for 2 h with [^{35}S]methionine. When combined in an integrated analysis the total rate of synthesis of p62$^{c\text{-}myc}$ and p60$^{c\text{-}myc}$ increased rapidly (less than 3 h) after serum stimulation and remained essentially constant for the entire length of the cell division cycle (Fig. 6). The integrated densitometric scan (Fig. 6B) was chosen to illustrate a consistent pattern of change in c-*myc* protein synthesis, because the relative rates of p60 and p62 synthesis (i.e., the ratio of the band intensities) were not consistent across experiments. We do not yet understand this variability in the p60/p62 ratio. In agreement with the parallel analysis of c-*myc* transcripts, no increase in c-*myc* protein synthesis could be found during S phase, nor during the G_1 period of the subsequent cell cycle (Fig. 6). The rate of synthesis of a 43-kDa protein associated nonspecifically with the immune complex served as a control for the changes observed in the

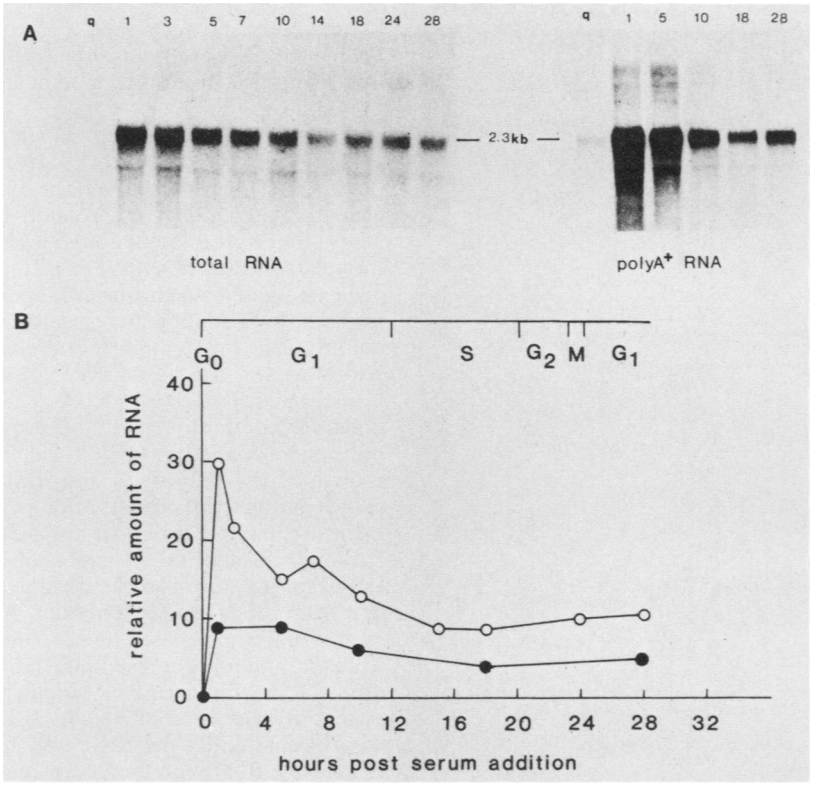

FIG. 5. Analysis of c-*myc* RNA during the cell cycle of mouse 3T3 cells. (A) Subconfluent, quiescent A31 3T3 cells (q) were stimulated by the addition of complete medium containing 10% calf serum. RNA was extracted at the times indicated above the gels (in hours) after the addition of serum and 10 μg of either total RNA or poly(A)$^+$ RNA purified by oligo(dT)cellulose chromatography was separated on a formaldehyde-agarose gel. The gel was blotted to nitrocellulose and hybridized to a nick-translated c-*myc* DNA probe, followed by autoradiography. (B) The relative amount of c-*myc* RNA at each time point was determined by densitometric scanning of the autoradiogram shown in panel A (○, total RNA; ●, poly(A)$^+$ RNA). The level of c-*myc* RNA in the quiescent cells was arbitrarily set at 1. Measured temporal subdividions of the cell cycle are indicated.

synthesis of c-*myc* proteins. Synthesis of this 43-kDa protein did not change during the entire cell cycle (Fig. 6B).

The high rate of synthesis of c-*myc* proteins in growing compared with quiescent cells (Fig. 3 and 6) implies that growing cells accumulate elevated levels of c-*myc* gene products. This conclusion, however, requires that the stability of the c-*myc* proteins does not change dramatically as quiescent cells are stimulated to grow. The stability of the c-*myc* protein therefore was analyzed in quiescent, serum-stimulated, and exponentially growing cells by a pulse-chase experiment. Mouse 3T3 cells were pulse-labeled for 2 h with [^{35}S]methionine, followed by a 6-h chase period in complete medium supplemented with unlabeled methionine. Cell extracts were prepared and immunoprecipitated with the c-*myc* antiserum. The p62$^{c\text{-}myc}$ protein was stable during the chase period, whereas p60$^{c\text{-}myc}$ disappeared completely during the chase (Fig. 6C). The same result was obtained for quiescent, serum-stimulated, and exponentially growing cells, suggesting that the stability of the c-*myc* proteins was similar in all phases of the cell cycle. However, a difference in the stability of the two c-*myc* proteins was observed: p62$^{c\text{-}myc}$ was significantly more stable than p60$^{c\text{-}myc}$ (Fig. 6C). A chase period including more time points revealed that the half-life of p60$^{c\text{-}myc}$ was about 2 h, whereas p62$^{c\text{-}myc}$ was stable for at least 6 h (data not shown).

DISCUSSION

c-*myc* is highly conserved in vertebrate evolution (7). Despite this sequence conservation, most of the antibodies raised against the human c-*myc* gene product fail to recognize c-*myc* proteins in other species (3, 21, 22; H. Persson et al., submitted for publication). In contrast, the antibody used in this study raised against a synthetic peptide internal to the amino-terminal portion of the human c-*myc* gene product has been shown to cross-react with proteins from distant species (34). Similarly, a peptide antiserum raised against the human c-*myc* gene product recently has been shown to immunoprecipitate mouse c-*myc* proteins with apparent molecular weights of 64,000 and 66,000 (38). In the present study, immunological, biochemical, and physiological evidence suggests that a major fraction of the mouse c-*myc* gene product is recognized by the heterospecific antibody used here. This antiserum immunoprecipitated both the 60- and 62-kDa components of the in vitro-synthesized mouse c-*myc* gene products. In addition, this antiserum recognized cell-derived proteins that shared molecular weights, isoelectric points, and pepsin-generated peptides with the in vitro-synthesized c-*myc* products (Fig. 2B). Finally, the rates of synthesis of p60$^{c\text{-}myc}$ and p62$^{c\text{-}myc}$ underwent changes that agreed closely with predictions from earlier studies of the c-*myc* transcripts. The inducibility by PDGF, the dependence on the growth state in A31 (but not in BPA31) cells, and the early increase during the G_0-G_1 transition in A31 cells have all been noted in previous studies (10, 26) and have been confirmed by the results of this study, which measured the accumulation of c-*myc* RNA and the rate of protein synthesis.

Thus, the data indicate that p60 and p62 are products of

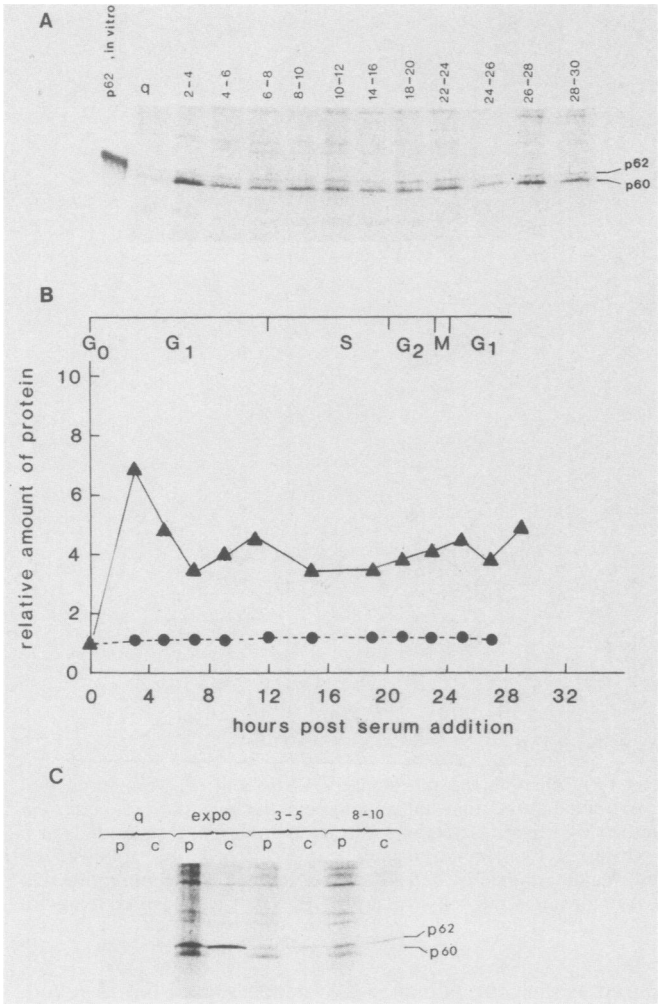

FIG. 6. Synthesis and stability of c-*myc* proteins during the growth cycle of mouse 3T3 cells. (A) Subconfluent quiescent (q) or serum-stimulated A31 cells were pulse-labeled for 2 h with [^{35}S]methionine (50 μCi/ml) at the times indicated above the gels (in hours) after serum restoration. Cell extracts containing equal amounts of acid-insoluble radioactivity were immunoprecipitated with a c-*myc* peptide antiserum followed by SDS-PAGE and fluorography. p62$^{c\text{-}myc}$ protein synthesized in vitro (Fig. 1) was used as a molecular weight marker in the gel. (B) Densitometric scanning of the fluorogram shown in panel A. The combined rate of synthesis of the c-*myc* proteins in quiescent cells was arbitrarily set at 1 (▲, integrated scan of both p60$^{c\text{-}myc}$ and p62$^{c\text{-}myc}$ combined; ●, p43, a nonspecifically immunoprecipitated cell cycle control). (C) 3T3 cells that were quiescent (q), exponentially growing (expo), or serum stimulated for 3 hours (3 to 5) or 8 hours (8 to 10) were pulse-labeled with [^{35}S]methionine for 2 h (p), followed by a 6-h chase in medium containing excess unlabeled methionine (c). Equal amounts of acid-insoluble radioactivity were immunoprecipitated with a c-*myc* peptide antiserum, followed by SDS-PAGE and fluorography.

the mouse c-*myc* gene that are expressed in 3T3 fibroblasts. The half-life of p62$^{c\text{-}myc}$ estimated in this study is longer than those recently reported for the short-lived human c-*myc* proteins (22, 38). This relatively long half-life of the p62$^{c\text{-}myc}$ protein therefore was unexpected. Although this discrepancy might suggest that p62 is not a product of the c-*myc* gene, we consider this possibility very unlikely for the reasons listed above. Furthermore, in support of the existence of long-lived c-*myc* proteins, we have detected four human c-*myc* proteins (p64, p65, p67, and p68) which, like the mouse c-*myc* proteins, have different half-lives as well as different posttranslational modifications (Persson et al., submitted).

Nontransformed BALB/c 3T3 mouse fibroblasts are convenient cells for the study of growth regulation by serum factors and therefore have been used in previous studies of growth-related c-*myc* expression (10, 26). In the present study, the expression of c-*myc* was monitored by measuring the relative rates of synthesis of the protein products of the gene in tightly synchronized subconfluent cells. This was achieved by combining the use of polylysine coating of the culture dishes with the use of medium that is similar to one which allows the serum-free growth of simian virus 40-transformed 3T3 cells (31, 40, 42). In agreement with the documented improvement of growth in low serum (31), polylysine coating extended the time required to achieve growth arrest. However, the inclusion of PPP instead of serum during the final starvation period permitted the attainment of complete arrest within 2 days, probably because of the absence of PDGF, a major mitogen for these cells (37). Polylysine coating also affected the kinetics of entry into and exit from S phase after quiescent A31 cells were stimulated with serum. Cells plated on uncoated dishes entered S phase 3 h later, and no decrease in the labeling index could be seen after 24 h, indicating a significant degradation of the synchrony observed on coated dishes. The superior attachment promoted by the basic polymer may make cells more responsive to growth factors or induce modifications in cell shape. Such changes could contribute to the differences in cell kinetics observed by us and others (6, 18). Purine supplementation has been shown to accelerate and sharpen the kinetics of entry into S phase in 3T3 cells (8, 17), and we have confirmed this effect (data not shown). In the medium that we used, the purine requirement is satisfied by the addition of Ham F12 medium, which contains hypoxanthine. The strategy described above allowed us to follow the cell cycle through mitosis and beyond, in contrast to methods that use confluent, density-arrested cells (36). Moreover, the new protocol resulted in tight synchrony without requiring the use of any chemical inhibitors.

This improved protocol for cell synchronization was used to study c-*myc* gene expression during the transition from the resting to the growing state and for more than one subsequent cell cycle. As also reported by others, the level of poly(A)$^+$ c-*myc* mRNA rapidly increased approximately 10-fold soon after quiescent cells were stimulated to reenter the cell cycle (Fig. 5). Similarly, the rates of synthesis of p60$^{c\text{-}myc}$ and p62$^{c\text{-}myc}$ increased sevenfold with the same kinetics (Fig. 6). About midway in G_1 (prereplicative phase) the expression of c-*myc* declined and reached a steady-state level that was maintained throughout the cell cycle and that corresponded to about five times the amount of mRNA and rate of protein synthesis observed in quiescent cells. These results indicate that expression of the c-*myc* gene is growth dependent but is not regulated in a cell cycle-specific manner. Deregulated expression of a gene, the products of which are required to initiate cell growth, could contribute to the establishment of the transformed phenotype. In agreement with this presumption, the rate of synthesis of c-*myc*-encoded proteins in the chemically transformed cell line BPA31 varied less than twofold when quiescent and growing cells were compared, a result that is consistent with the previous analysis of RNA made under similar conditions (10).

The stability of the c-*myc*-encoded proteins did not change

significantly when quiescent cells were stimulated to reenter the growth cycle (Fig. 6C), suggesting that serum stimulation rapidly increases the accumulation of c-*myc* gene products. The half-life of $p62^{c\text{-}myc}$ was, however, much longer than that of $p60^{c\text{-}myc}$. In pulse-chase experiments, the latter protein decayed with a half-life of about 2 h. The difference in stability between $p62^{c\text{-}myc}$ and $p60^{c\text{-}myc}$ was also apparent after prolonged labeling of cells with [^{35}S]methionine. In agreement with the pulse-chase analysis, the quantity of radioactivity incorporated into $p62^{c\text{-}myc}$ was always increased by extending the labeling period, indicating further that this protein is stable. In contrast, the amount of $p60^{c\text{-}myc}$ was greatly reduced under these conditions, and the maximum quantity of label incorporated into $p60^{c\text{-}myc}$ was obtained with a labeling time of 2 h. This result is consistent with the instability of $p60^{c\text{-}myc}$ demonstrated by pulse-chase analysis.

As shown here for the c-*myc* proteins, heterogeneity in the product of another oncogene (c-*fos*) has recently been demonstrated. Four c-*fos* proteins ranging in molecular weight from 56,000 to 72,000 have been identified with different anti-c-*fos* sera (13, 27, 32). These different forms of the c-*fos* proteins are modified posttranslationally and also decay at different rates (27, 32). Similarly, there may also be additional forms of the mouse c-*myc* protein that are not recognized by the human peptide antiserum used in our studies.

Like the c-*myc* gene products, the c-*fos* proteins, as well as the cellular antigen p53, are nuclear proteins, the rates of synthesis of which are increased after serum stimulation of quiescent cells (20, 27, 32, 39). They therefore may play important roles either in the transition of cells from the resting to the actively growing state or in discrete transitions internal to the cell cycle of proliferating cells. The induction of c-*fos* protein synthesis has a greater amplitude and occurs earlier than the increase in the rate of synthesis of $p60^{c\text{-}myc}$ and $p62^{c\text{-}myc}$ following serum stimulation (27, 32). In contrast to the periodic fluctuation of c-*fos* expression (20, 27, 32), synthesis of c-*myc*-encoded proteins continues at an elevated rate throughout the cell cycle, suggesting that functional c-*myc* gene products are required during all phases of the cell cycle. Two articles addressing the relation of c-*myc* gene expression to the cell cycle have recently appeared (23, 47). These authors have reported constant levels of c-*myc* RNA and c-*myc* protein synthesis during the growth-division cycle of human and avian, normal and transformed exponentially growing cells that were fractionated on the basis of cell size (and hence stage of cell cycle) by centrifugal elutriation. These results agree with our conclusion that c-*myc* expression does not vary across the cell cycle and, in particular, during G_1 or S phase. However, discrepancies with our results still remain concerning the level of down regulation of c-*myc* expression subsequent to growth arrest. It should be noted that, like the BPA31 cells used in our experiments, some of the cells used by these authors were also transformed, and hence potentially quite different from normal cells in the control of c-*myc* expression.

ACKNOWLEDGMENTS

We thank Robert Curtin for excellent technical assistance. We are grateful to Robert Croy and Oreste Acuto for assistance and to Judith Campisi, Arthur B. Pardee, and Philip Leder for many helpful discussions.

H.P. was supported by a European Molecular Biology Organization Fellowship, and H.E.G. was supported by a Tumor Biology Training Grant from the National Institutes of Health to the Dana-Farber Cancer Institute. F.G. was supported in part by Institut National de la Santé et de la Recherche Médicale (France), by a BRSG grant to the Dana-Farber Cancer Institute, and by a short-term European Molecular Biology Organization Fellowship. This research was supported by Public Health Service grant GM CA 24571 from the National Institutes of Health to Arthur B. Pardee, Dana-Farber Cancer Institute, and by grants from the American Business for Cancer Research Foundation and the E. I. DuPont de Nemours & Co., Inc., to Philip Leder, Department of Genetics, Harvard Medical School.

LITERATURE CITED

1. **Abrams, H. D., L. R. Rohrschneider, and R. N. Eisenman.** 1982. Nuclear location of the putative transforming protein of avian myelocytomatosis virus. Cell **29**:427–439.
2. **Acuto, O., R. E. Hussey, K. A. Fitzgerald, J. P. Protentis, S. C. Meuer, S. F. Schlossman, and E. L. Reinherz.** 1983. The human T cell receptor: appearance in ontogeny and biochemical relationship of α and β subunits on IL-2 dependent clones and T cell tumors. Cell **34**:717–726.
3. **Alitalo, K., G. Ramsay, J. M. Bishop, S. O. Pfeifer, W. W. Colby, and A. D. Levinson.** 1983. Identification of nuclear proteins encoded by viral and cellular myc oncogenes. Nature (London) **306**:274–277.
4. **Armelin, H. A., M. C. S. Armelin, K. Kelly, T. Stewart, P. Leder, B. H. Cochran, and C. D. Stiles.** 1984. Functional role for c-myc in mitogenic response to platelet-derived growth factor. Nature (London) **310**:655–660.
5. **Aviv, H., and P. Leder.** 1972. Purification of biologically active globin messenger RNA by chromatography on oligothymidylic acid-cellulose. Proc. Natl. Acad. Sci. USA **69**:1408–1412.
6. **Ben-Ze'ev, A., S. R. Farmer, and S. Penman.** 1980. Protein synthesis requires cell-surface contact while nuclear events respond to cell shape in anchorage-dependent fibroblasts. Cell **21**:365–372.
7. **Bishop, J. M.** 1983. Cellular oncogenes and retroviruses. Annu. Rev. Biochem. **52**:301–354.
8. **Brooks, R. F.** 1975. The kinetics of serum-induced initiation of DNA synthesis in BHK 21/C13 cells, and the influence of exogenous adenosine. J. Cell. Physiol. **86**:369–378.
9. **Bunte, T., P. Donner, E. Pfaff, B. Reis, I. Greiser-Wilke, H. Schaller, and K. Moelling.** 1984. Inhibition of DNA binding of purified $p55^{v\text{-}myc}$ in vitro by antibodies against bacterially expressed myc protein and a synthetic peptide. EMBO J. **3**:1919–1924.
10. **Campisi, J., H. E. Gray, A. B. Pardee, M. Dean, and G. E. Sonenshein.** 1984. Cell cycle control of c-myc but not c-ras expression is lost following chemical transformation. Cell **36**:241–247.
11. **Chirgwin, J., A. Aeyble, R. McDonald, and W. Rutter.** 1979. Isolation of biologically active ribonucleic acid from sources enriched in ribonuclease. Biochemistry **18**:5294–5299.
12. **Collins, S., and M. Groudine.** 1982. Amplification of endogenous myc-related DNA sequences in a human myeloid leukemia cell line. Nature (London) **298**:679–681.
13. **Curran, T., A. D. Miller, L. Zokas, and I. M. Verma.** 1984. Viral and cellular fos proteins: a comparative analysis. Cell **36**:259–268.
14. **Dalla-Favera, R., F. Wong-Staal, and R. C. Gallo.** 1982. Onc gene amplification in promyelocytic leukemia cell line HL-60 and primary leukemic cells of the same patient. Nature (London) **299**:61–63.
15. **Donner, P. I., I. Greiser-Wilke, and K. Moelling.** 1982. Nuclear localization of DNA binding of the transforming gene product of arian myelocytomatosis virus. Nature (London) **296**:262–266.
16. **Eisenman, R. N., C. Y. Tachibana, H. D. Abrams, and S. R. Hann.** 1985. v-myc and c-myc encoded proteins are associated with the nuclear matrix. Mol. Cell. Biol. **5**:114–126.
17. **Engström, W., and A. Zetterberg.** 1984. The relationship between purines, pyrimidines, nucleosides, and glutamine for fibroblast cell proliferation. J. Cell. Physiol. **120**:233–241.
18. **Folkman, J., and A. Moscona.** 1978. Role of cell shape in growth control. Nature (London) **273**:345–349.

19. **Green, M. R., T. Maniatis, and D. A. Melton.** 1983. Human β-globin pre-mRNA synthesized in vitro is accurately spliced in Xenopus oocyte nuclei. Cell **32**:681–694.
20. **Greenberg, M. E., and E. B. Ziff.** 1984. Stimulation of 3T3 cells induces transcription of the c-fos proto-oncogene. Nature (London) **311**:433–438.
21. **Hann, S. R., H. D. Abrams, L. R. Rohrschneider, and R. N. Eisenman.** 1983. Proteins encoded by the v-myc and c-myc oncogenes: identification and localization in acute leukemia virus transformants and bursal lymphoma cell lines. Cell **34**:789–798.
22. **Hann, S. R., and R. N. Eisenman.** 1984. Proteins encoded by the human c-myc oncogene: differential expression in neoplastic cells. Mol. Cell. Biol. **4**:2486–2497.
23. **Hann, S. R., C. B. Thompson, and R. N. Eisenman.** 1985. c-myc oncogene protein synthesis is independent of the cell cycle in human and avian cells. Nature (London) **314**:366–369.
24. **Hayward, W. S., B. G. Neel, and S. M. Astrin.** 1981. Activation of a cellular onc gene by promoter insertion in ALV-induced lymphoid leukosis. Nature (London) **290**:475–480.
25. **Holley, R. W., J. H. Baldwin, J. A. Kiernan, and T. O. Messmer.** 1976. Control of growth of benzo(a)pyrene-transformed 3T3 cells. Proc. Natl. Acad. Sci. USA **73**:3229–3232.
26. **Kelly, K., B. H. Cochran, C. H. Stiles, and P. Leder.** 1983. Cell-specific regulation of the c-myc gene by lymphocyte mitogens and platelet-derived growth factor. Cell **35**:603–610.
27. **Kruijer, W., J. A. Cooper, T. Hunter, and I. M. Verma.** 1984. Platelet-derived growth factor induces rapid but transient expression of the c-fos gene and protein. Nature (London) **312**:711–716.
28. **Land, H., L. F. Parada, and R. A. Weinberg.** 1983. Tumorigenic conversion of primary embryo fibroblasts requires at least two cooperating oncogenes. Nature (London) **304**:596–602.
29. **Leder, P., J. Battey, G. Lenoir, C. Moulding, W. Murphy, H. Potter, T. Stewart, and R. Taub.** 1983. Translocations among antibody genes in human cancer. Science **222**:766–771.
30. **Little, C. D., M. M. Nau, D. N. Carney, A. F. Gazdar, and J. D. Minna.** 1983. Amplification and expression of the c-myc oncogene in human lung cancer cell lines. Nature (London) **306**:194–196.
31. **McKeehan, W. L., and R. G. Ham.** 1976. Stimulation of clonal growth of normal fibroblasts with substrata coated with basic polymers. J. Cell. Biol. **71**:727–734.
32. **Muller, R., R. Bravo, J. Burckhardt, and T. Curran.** 1984. Induction of c-fos gene and protein by growth factors precedes activation of c-myc. Nature (London) **312**:716–720.
33. **O'Farrell, P. H.** 1975. High resolution two dimensional electrophoresis of proteins. J. Biol. Chem. **250**:4007–4021.
34. **Persson, H., L. Hennighausen, R. Taub, W. DeGrado, and P. Leder.** 1984. Antibodies to human c-myc oncogene product: evidence of an evolutionarily conserved protein during cell proliferation. Science **225**:687–693.
35. **Persson, H., and P. Leder.** 1984. Nuclear localization and DNA binding properties of protein expressed by human c-myc oncogene. Science **225**:718–721.
36. **Pledger, W. J., C. D. Stiles, H. N. Antoniades, and C. D. Scher.** 1977. Induction of DNA synthesis in BALB/c 3T3 cells by serum components: reevaluation of the commitment process. Proc. Natl. Acad. Sci. USA **74**:4481–4485.
37. **Pledger, W. J., C. D. Stiles, H. N. Antoniades, and C. D. Scher.** 1978. An ordered sequence of events is required before BALB/c 3T3 cells become committed to DNA synthesis. Proc. Natl. Acad. Sci. USA **75**:2839–2843.
38. **Ramsay, G., G. I. Evan, and J. M. Bishop.** 1984. The protein encoded by the proto-oncogene c-myc. Proc. Natl. Acad. Sci. USA **81**:7742–7746.
39. **Reich, N. C., and A. G. Levine.** 1984. Growth regulation of a cellular tumour antigen, p53, in nontransformed cells. Nature (London) **308**:199–201.
40. **Rockwell, G., G. Sato, and D. McClure.** 1980. The growth requirement of SV40-transformed Balb/c 3T3 cells in serum-free monolayer culture. J. Cell. Physiol. **103**:323–331.
41. **Schneider, E. L., E. J. Stanbridge, and C. J. Epstein.** 1974. Incorporation of (^{3}H)uridine and (^{3}H)uracil into RNA: a simple technique for the detection of mycoplasma contamination of cultured cells. Exp. Cell Res. **84**:311–318.
42. **Shipley, G. D., and R. G. Ham.** 1983. Multiplication of Swiss 3T3 cells in serum-free medium. Exp. Cell Res. **146**:249–260.
43. **Stanton, L. W., R. Watt, and K. B. Marcu.** 1983. Translocation, breakage and truncated transcripts of c-myc oncogene in murine plasmacytomas. Nature (London) **303**:401–406.
44. **Stein, G. H., and R. Yanishevsky.** 1979. Autoradiography. Methods Enzymol. **58**:279–292.
45. **Stewart, T. A., A. R. Bellvé, and P. Leder.** 1984. Transcription and promoter usage of the myc gene in normal and spermatogenic cells. Science **226**:707–710.
46. **Stewart, T. A., P. K. Pattengale, and P. Leder.** 1984. Spontaneous mammary adenocarcinomas in transgenic mice that carry and express MTV/myc fusion genes. Cell **38**:627–637.
47. **Thompson, C. B., P. B. Challoner, P. E. Neiman, and M. Groudine.** 1985. Levels of c-myc oncogene mRNA are invariant throughout the cell cycle. Nature (London) **314**:363–366.